Latent Olefin Metathesis Catalysts Featuring Chelating Alkylidenes

Andrew Hejl, Michael W. Day, and Robert H. Grubbs*

The Arnold and Mabel Beckman Laboratories of Chemical Synthesis, Division of Chemistry and Chemical Engineering, California Institute of Technology, Pasadena, California 91125

Received July 11, 2006

The synthesis of a series of ruthenium-based metathesis catalysts featuring imine donors chelated through the alkylidene group is described. The relative placement of the imine carbon−nitrogen double bond (exocyclic vs endocyclic) has a major impact on the initiation behavior. When used in metathesis applications, catalysts with an endocyclic imine bond show latent behavior and a high degree of tunability. The incorporation of additional donor atoms is an additional strategy for controlling initiation behavior. These latent catalysts could be useful in high-temperature applications.

Introduction

In recent years olefin metathesis has become a widely used method for the formation of carbon−carbon bonds in organic synthesis and polymer chemistry.[1] The development of well-defined transition metal complexes capable of catalyzing this transformation has been particularly important in expanding the utility of this reaction.[2] A great deal of effort has been focused on ruthenium-based catalysts because of their increased environmental tolerance relative to molybdenum-based systems.[3] The incorporation of N-heterocyclic carbene (NHC) ligands in ruthenium catalysts, such as H_2IMes (H_2IMes = 1,3-dimesitylimidazolidine-2-ylidene), has led to catalysts **1**−**3** (Chart 1), which show high activity and fast initiation in a range of metathesis reactions.[4]

For some processes it is desirable that catalyst initiation be controllable. For example, efficient ring-opening metathesis polymerization (ROMP) reactions require adequate mixing of monomer and catalyst before polymerization occurs. For these applications, catalysts that initiate polymerization at a high rate only upon heating would be desirable. However, both **1** and **2** are competent metathesis catalysts at or below room temperature and so, alone, are not well suited for applications where catalyst latency is beneficial.

Experimental studies have shown that, for the majority of ruthenium catalysts, dissociation of a donor ligand provides entry to the catalytic cycle.[5] We felt that, of a number of possibilities, tethering a donor ligand to the ruthenium center via the alkylidene group was the most attractive method to afford latent catalysts. If the donor ligand, L, is attached to the alkylidene, the chelate effect favors the precatalyst over the metathesis active form (eq 1). However, after a catalytic turnover, the donor will no longer be tethered and catalysis should proceed quickly. This switch in catalyst structure from chelated to nonchelated once catalysis begins makes this a more attractive method for designing thermally latent catalysts than other strategies, such as other bidentate chelates[6] or addition of excess phosphine to a standard catalyst such as **1**.[7] These other methods will frequently result in catalysts with a decreased overall efficiency, but this limitation can hopefully be overcome by using a chelated donor.

Chart 1. Commonly Used Olefin Metathesis Catalysts

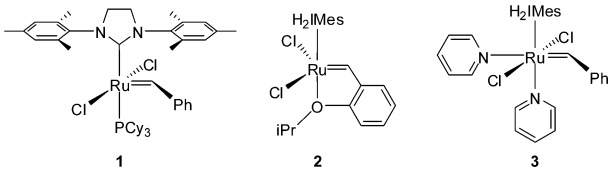

1 **2** **3**

Chart 2. Previous Examples of Metathesis Catalysts with Chelated Alkylidenes

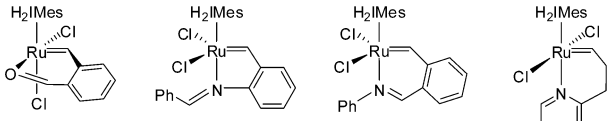

4 **5** **6** **7**

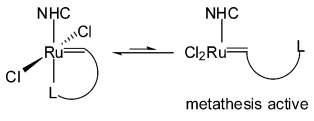

(1)

While catalyst **2** features a chelating oxygen donor, this catalyst is active below room temperature, suggesting that the ether is not strong enough to render **2** latent.[8] The addition of electron-donating groups to **2** has been applied by Grela and co-workers to render this family of catalysts thermally switchable.[9] Fürstner and co-workers as well as Slugovc and co-

* Corresponding author. E-mail: rhg@caltech.edu.

(1) Grubbs, R. H., Ed. *Handbook of Metathesis*; Wiley-VCH: Weinheim, 2003.

(2) Trnka, T. M.; Grubbs, R. H. *Acc. Chem. Res.* **2001**, *34*, 18−29.

(3) Schrock, R. R.; Hoveyda, A. H. *Angew. Chem. Int. Ed.* **2003**, *42*, 4592−4633.

(4) (a) Scholl, M.; Ding, S.; Lee, C. W.; Grubbs, R. H. *Org. Lett.* **1999**, *1*, 953−956. (b) Garber, S. B.; Kingsbury, J. S.; Gray, B. L.; Hoveyda, A. H. *J. Am. Chem. Soc.* **2000**, *122*, 8168−8179. (c) Gessler, S.; Randl, S.; Blechert, S. *Tetrahedron Lett.* **2000**, *41*, 9973−9976. (d) Sanford, M. S.; Love, J. A.; Grubbs, R. H. *Organometallics* **2001**, *20*, 5314−5318.

(5) (a) Sanford, M. S.; Ulman, M.; Grubbs, R. H. *J. Am. Chem. Soc.* **2001**, *123*, 749−750. (b) Sanford, M. S.; Love, J. A.; Grubbs, R. H. J. *Am. Chem. Soc.* **2001**, *123*, 6543−6554.

(6) (a) Chang, S.; Jones, L., II; Wang, C.; Henling, L. M.; Grubbs, R. H. *Organometallics* **1998**, *17*, 3460−3465. (b) DeClercq, B.; Verpoort, F. *Tetrahedron Lett.* **2002**, *43*, 9101−9104. (c) Denk, K.; Fridgen, J.; Herrmann, W. A. *Adv. Synth. Catal.* **2002**, *344*, 666−670.

(7) For a more complete discussion of the various strategies for designing latent metathesis catalysts see ref 11.

(8) Michrowska, A.; Bujok, R.; Harutyunyan, S.; Sashuk, V.; Dolgonos, G.; Grela, K. *J. Am. Chem. Soc.* **2004**, *126*, 9318−9325.

(9) Gulajski, L.; Michrowska, A.; Bujok, R.; Grela, K. *J. Mol. Catal. A* **2006**, *254*, 118−123.

10.1021/om060620u CCC: $33.50
Publication on Web 11/14/2006

workers have reported catalysts featuring ester- or aldehyde-substituted benzylidenes (**4**) that show reduced activity at room temperature.[10] They have also examined imine-containing systems (**5** and **6**) based on a similar aryl framework and identified differences in catalysis with varying chelate ring sizes.[11] We have employed the 2-(3-butenyl)pyridine ligand, originally described by van der Schaaf and co-workers on phosphine systems,[12] to synthesize latent pyridine-containing catalysts based on the H_2IMes framework (**7**).[13] In these compounds pyridines, which are weakly bound, fast-dissociating ligands when not chelated, provided latent catalysts when tethered to the alkylidenes. Additionally, pyridine was found to bind in two geometries (cis or trans to the NHC), providing catalysts that showed very different initiation patterns.[14] Attempts to modify initiation behavior by varying the steric and electronic parameters on the pyridine ring were met with limited success. We felt that moving to an imine framework with an alkylidene tether offered great potential to vary the steric and electronic environment on the imine nitrogen.

In this report, we describe the synthesis and catalytic behavior of ruthenium alkylidenes that contain an NHC ligand and an imine donor tethered to the alkylidene. We have examined the effect of changing the relative placement of the imine bond (endocyclic vs exocyclic) and also the incorporation of an additional potential donor ligand. These imine-based systems afford latent metathesis catalysts with a high degree of tunability of initiation behavior.

Results and Discussion

Exocyclic Imine Catalysts. The imine ligands **8a**,**b** were prepared by simple condensation of 2,2-dimethyl-4-pentenylamine with various aldehydes. The resulting unsaturated imines could then be reacted with $(H_2IMes)(py)_2(Cl)_2Ru{=}CHPh$ (**3**) at room temperature to afford the imine-bound catalysts ($(H_2IMes)(Cl)_2Ru(\kappa^2\text{-}(C,N)CHCH_2CMe_2CH_2N{=}CHR)$) (**9a**,**b**) in good yields (eq 2). Complex **3** was chosen as a catalyst precursor because the lability of the pyridine ligands allowed for fast ligand substitution and metathesis.[4d] The resulting imine-bound catalysts **9a**,**b** were isolated by simple precipitation on the benchtop. The complexes could be purified by column chromatography with minimal decomposition during this process.

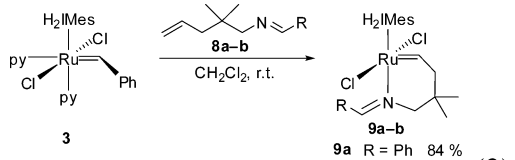

(2)

The ^{1}H NMR spectra for **9a**,**b** are consistent with the symmetric C_s structure shown in eq 2. The alkylidene proton resonance is especially diagnostic, appearing between 18.5 and 18.7 ppm as a triplet coupled to the adjacent methylene protons.

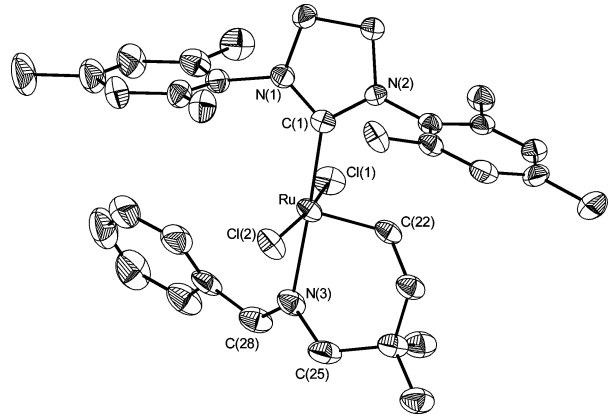

Figure 1. Solid-state structure of **9a** with thermal ellipsoids drawn at 50% probability. Selected bond distances (Å) and angles (deg): Ru−C(1) = 2.052(4), Ru−C(22) = 1.814(4), Ru−N(3) = 2.167(3), Ru−Cl(1) = 2.3905(10), Ru−Cl(2) = 2.3783(10), Cl(1)−Ru−Cl(2) = 169.42(4), C(1)−Ru−N(3) = 176.97(13), C(22)−Ru−N(3) = 87.76(15).

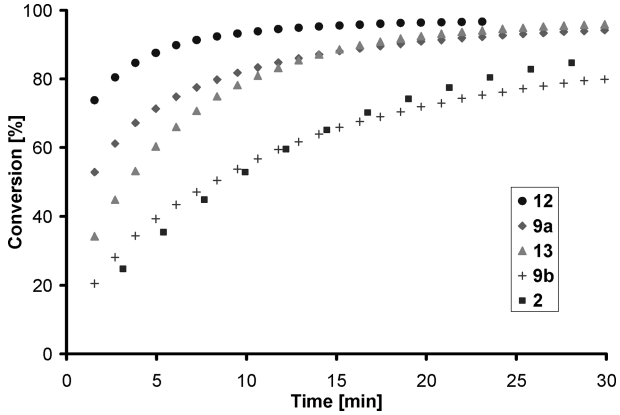

Figure 2. Conversion plot for RCM of **10** with **2**, **9a**,**b**, **12**, and **13** (2.5 mol %, 10 °C, C_6D_6).

The ^{13}C NMR spectrum shows the alkylidene carbon shifted very far downfield (~341−343 ppm), while the NHC carbon appears near 218 ppm. There is no indication of side-bound coordination of the imine nitrogen, as was the case with chelating pyridines or benzoate esters.[10,13]

Crystals suitable for X-ray analysis were obtained for **9a**, and the resulting structure is shown in Figure 1. The complex displays the typical distorted square pyramidal geometry for five-coordinate ruthenium alkylidenes. The Ru−N bond length (2.167(3) Å) is shorter than in the bispyridine precursor **3** (2.203(3) Å), consistent with stronger ligand binding. The benzaldimine portion is directed up into the empty quadrant trans to the alkylidene group, a feature also observed by Slugovc for complex **5**.[11] This placement of the phenyl ring maintains the more energetically stable *E*-imine conformation but may result in an unfavorable steric interaction with the $RuCl_2$ plane (the Cl−Ru−Cl angle is widened to 169.42(4)°).

Complexes **9a**,**b** were tested for catalytic activity in the ring-closing metathesis (RCM) of diethyldiallyl malonate (**10**) (eq 3) and found to be extremely active catalysts. When the reaction was performed at 30 °C with **9a**, 90% conversion was reached within 2 min. In fact, **9a** is certainly not a latent catalyst and behaves much more like **2**, displaying activity below room temperature. Figure 2 compares the performance of **9a**,**b** with **2** and two derivatives of **2** (**12** and **13**, Chart 3), which were specially engineered to improve the initiation behavior of that

(10) (a) Fürstner, A.; Thiel, O. R.; Lehmann, C. W. *Organometallics* **2002**, *21*, 331−335. (b) Slugovc, C.; Perner, B.; Stelzer, F.; Mereiter, K. *Organometallics* **2004**, *23*, 3622−3626.

(11) Slugovc, C.; Burtscher, D.; Stelzer, F.; Mereiter, K. *Organometallics* **2005**, *24*, 2255−2258.

(12) van der Schaaf, P. A.; Kolly, R.; Kirner, H.-J.; Rime, F.; Mühlebach, A.; Hafner, A. *J. Organomet. Chem.* **2000**, *606*, 65−74.

(13) Ung, T.; Hejl, A.; Grubbs, R. H.; Schrodi, Y. *Organometallics* **2004**, *23*, 5399−5401.

(14) Grela and co-workers have recently reported quinoline-derived catalysts that exhibit a similar cis/trans isomerization behavior. Barbasiewicz, M.; Szadkowska, A.; Bujok, R.; Grela, K. *Organometallics* **2006**, *25*, 3608−3613.

Chart 3. Fast Initiating Variants of 2

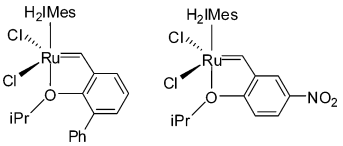

family of catalysts.[15] **9a** compares favorably to the fast-initiating variants, while **9b** shows similar activity to **2** in this reaction. In these cases, the initiation behavior is the most likely source of variation since the nondissociating portion remains the same.

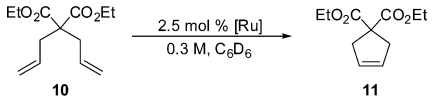

(3)

Endocyclic Imine Catalysts. We were interested in whether changing the placement of the imine bond from an exocyclic to an endocyclic position might result in a catalyst with a slower initiation rate. Other researchers have reported that changing the chelate ring size has resulted in large differences in catalyst behavior; however in their study the imine bond was also changed from an exocyclic to an endocyclic placement.[11] To separate these effects, we adapted our catalyst framework to result in an endocyclic imine bond, while maintaining the same six-membered chelate ring size.

The imine ligands **14a**−**e** were prepared by condensation of commercially available 2,2-dimethyl-4-pentenal with the corresponding primary amine. The ligands were designed with the gem-dimethyl substituents for two reasons: to stabilize the chelated product by the Thorpe−Ingold effect[16] and, more importantly, to prevent formation of enamines, which are known to react to form catalytically inactive Fischer carbenes.[17] The catalysts were synthesized in good yields by reaction of the imine ligands with **3** (eq 4). The resulting imine-bound compounds **15a**−**e** could be isolated by precipitation on the benchtop and easily purified by column chromatography, without decomposition, to give stable pale green solids. Alternatively, the synthesis could be carried out from **1**, but this reaction required heating and longer reaction times.

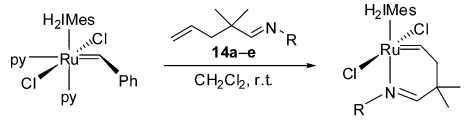

15a R = Ph 83 %
15b R = ^{i}Pr 80 %
15c R = Cy 84 %
15d R = ^{t}Bu 56 %
15e R = Me 84 %
(4)

The ^{1}H NMR spectra for **15a**−**e** were similar to those observed for **9a**−**e**. The characteristic downfield alkylidene proton was split into a triplet by coupling to the adjacent methylene. Another interesting feature of the spectra is that resonances corresponding to the H_2IMes ligand are affected by the nature of the imine substituent. Groups with small steric profiles like phenyl (**15a**) and methyl (**15e**) display very sharp ^{1}H NMR resonances for both the NHC backbone protons and mesityl peaks. For larger groups (e.g., *tert*-butyl, **15d**) the ^{1}H NMR resonances for the NHC protons are significantly broadened. The more sterically demanding groups may hinder free rotation of the NHC, causing several protons on the H_2IMes ligand to appear as discrete resonances.[18] Though some catalysts show a more symmetric environment than others, there is again no indication of side-bound coordination of the imine nitrogen.

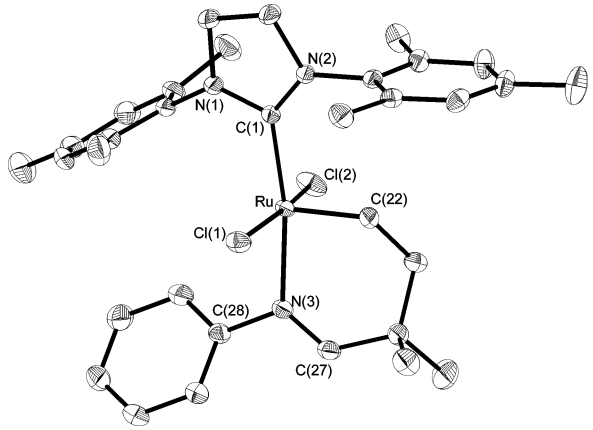

Figure 3. Solid-state structure of **15a** with thermal ellipsoids drawn at 50% probability. Selected bond distances (Å) and angles (deg): Ru−C(1) = 2.0387(14), Ru−C(22) = 1.8100(15), Ru−N(3) = 2.1488(12), Ru−Cl(1) = 2.3788(4), Ru−Cl(2) = 2.3759(4), Cl(1)−Ru−Cl(2) = 167.674(15), C(1)−Ru−N(3) = 169.94(5), C(22)−Ru−N(3) = 89.67(6).

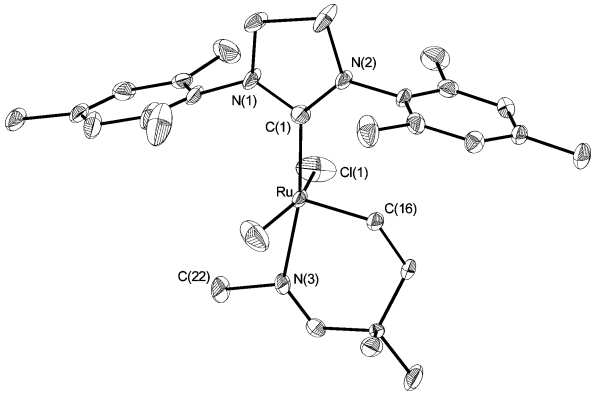

Figure 4. Solid-state structure of **15e** with thermal ellipsoids drawn at 50% probability. Selected bond distances (Å) and angles (deg): Ru−C(1) = 2.020(3), Ru−C(16) = 1.808(3), Ru−N(3) = 2.118(3), Ru−Cl(1) = 2.3488(9), Cl(1)−Ru−Cl(1)* = 162.28(4), C(1)−Ru−N(3) = 169.66(10), C(16)−Ru−N(3) = 89.71(12) (*symmetry generated).

The symmetric nature of the resulting endocyclic imine compounds was confirmed by solid-state structural studies. Crystals suitable for X-ray analysis were obtained for catalysts **15a** and **15e** and are shown in Figures 3 and Figure 4, respectively. The Ru−N bond lengths in **15a** and **15e** (2.149(1) and 2.118(3) Å) are shorter than in **9a**, suggesting a stronger interaction with the ruthenium for the endocyclic imine donors. The more electron-donating and less sterically demanding methyl substituent displays a shorter Ru−N bond. Additionally the Cl−Ru−Cl bond angles also reflect differences in the nitrogen substituents, as the bonds in **15e** are compressed compared with those in **15a** (162.28(4)° vs 167.67(2)°), likely a result of the lower steric demands of the methyl substituent.

The imine ligand provides a good handle for IR spectroscopy, in this case one directly involved in the metal binding. The C=

(15) (a)Wakamatsu, H.; Blechert, S. *Angew. Chem. Int. Ed.* **2002**, *41*, 2403−2405. (b) Grela, K.; Harutyunyan, S.; Michrowska, A. *Angew. Chem. Int. Ed.* **2002**, *41*, 4038−4040.

(16) Allinger, N. L.; Zalkow, V. *J. Org. Chem.* **1960**, *25*, 701−704.

(17) Zhang, J.; Gunnoe, T. B. *Organometallics* **2003**, *22*, 2291−2297.

(18) Sanford, M.S. Ph.D. Thesis, California Institute of Technology, 2001.

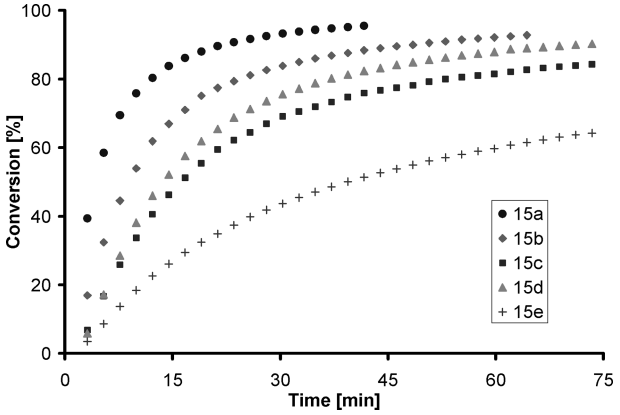

Figure 5. Conversion plot for RCM of **10** with **15a**−**e** (2.5 mol %, 40 °C, C_6D_6).

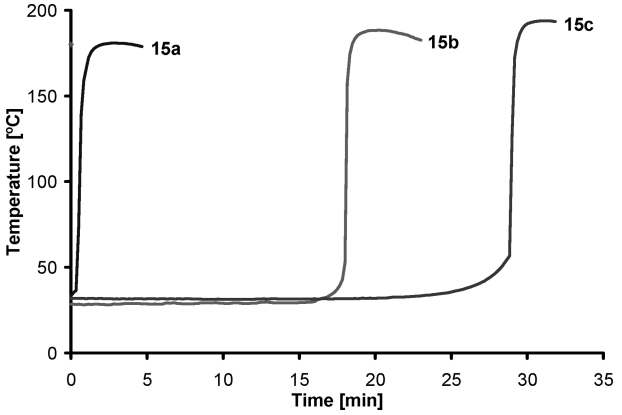

Figure 6. Exotherm plot for ROMP of DCPD with **15a**−**c** (30 000:1 M/C, 30 °C).

Table 1. IR Data for Imine $\nu_{C=N}$ Stretch (cm^{-1}) in Free Ligands (14) and Catalysts (15)

imine substituent	$\nu_{C=N}$ [**14**]	$\nu_{C=N}$ [**15**]	$\Delta\nu_{C=N}$
a, R = Ph	1648.0	1634.3	13.7
b, R = ^{i}Pr	1661.4	1642.6	18.8
c, R = Cy	1662.7	1641.1	21.6
d, R = ^{t}Bu	1665.9	1638.6	27.3
e, R = Me	1670.9	1635.4	35.5

N stretching frequencies were measured for the free ligands (**14a**−**e**) and the corresponding ruthenium complexes (**15a**−**e**), and the results are listed in Table 1. All catalysts show a decrease in the energy of the C═N stretch, indicating a weakening of the bond. This effect could result from π-back-bonding from the ruthenium into the C═N π^* orbital or from binding of the metal forcing the imine out of its ideal conformation, thus weakening the bond. The magnitude of the shift of the $\nu_{C=N}$ also correlates with the expected strength of the Ru−N interaction. The more tightly bound imine in **15e** shows the greatest shift, while the less donating ligand in **15a** shows the smallest shift in energy.

Complexes **15a**−**e** were tested for activity in the RCM of **10** at elevated temperature (eq 3). Figure 5 shows the progress of the reaction when carried out at 40 °C. This reaction is complete (>95%) within 5−10 min when performed with **1** or **2**. All complexes examined catalyzed this reaction to completion with an order of activity **9a** > **9b** > **9d** > **9c** > **9e** (in Figure 5 only the first 75 min of reaction time are shown, not the entire reaction to completion). These results are consistent with the relative donating ability/steric demand of the imine substituents: the electron-poor phenyl substituent is the fastest, while the small methyl group shows the slowest reaction. This order of activity also correlates well with the magnitude of the shift in $\nu_{C=N}$ measured by IR spectroscopy (Table 1). To assess the latency of these catalysts, the RCM of **10** was studied under standard reaction conditions and referenced to **1** and **2** (1 mol %, CD_2Cl_2, 30 °C).[19] **15a** and **15e** showed dramatically reduced activity compared to **1** and **2** near room temperature, confirming their latency (see Supporting Information for details).

To evaluate catalyst behavior in polymerization reactions, these complexes were tested in the ROMP of dicyclopentadiene (DCPD) (eq 5). Figure 6 shows an exotherm graph of DCPD ROMP started at 30 °C for catalysts **15a**−**c**. In these experiments, the catalyst is added to a sample of DCPD held in a constant-temperature oil bath monitored with a thermocouple. As the strained norbornene-like double bond is opened, energy is released that heats the system, eventually resulting in a sharp rise in temperature. The resulting plots contain information about two factors: initiation rate (time to exotherm) and activity (peak temperature). This reaction is particularly useful for latent systems, because for active catalysts, such as **1** and **2**, the reaction occurs very quickly, leading to microencapsulation of the catalyst and incomplete polymerization. When tested with catalysts **15a**−**c**, microencapsulation is avoided and complete incorporation of DCPD into the polymer was observed. Notable about these graphs is that the trend observed in the RCM data is reflected in the ROMP of DCPD, with the fastest initiating catalyst, **15a**, showing the shortest time to exotherm. Additionally, the catalysts surveyed show similar peak temperatures, as expected for systems all based on the H_2IMes framework. All catalysts show almost an "on/off" polymerization behavior, without an extended, gradual rise in temperature before the onset of polymerization. This should allow for an educated choice of catalyst to control the time to exotherm while avoiding slow, inefficient polymerization.

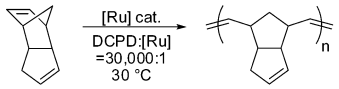

(5)

The very different initiation behavior of **15a** when compared with **9a** shows that the relative placement of the imine C═N bond has a large effect on catalyst activity. In this case vastly different activities are observed in spite of the identical chelate ring size. It is possible that the exocyclic imine framework examined here disrupts the Ru−N bonding through a steric interaction with the rest of the catalyst framework. The weakening of the Ru−N bond results in a more efficient initiator and ultimately leads to higher activity. An earlier report ascribed the differences in initiation rates of **4** and **5** to the varying chelate ring sizes,[11] but the data reported here indicate that the placement of the imine bond has a huge impact on activity.

3-Point Catalysts. The development of a simple, modular synthesis of unsaturated imine ligands has also enabled us to examine other related catalyst design motifs. We were interested in synthesizing catalysts that incorporate two potential donor ligands tethered through the alkylidene group. This would set up a 3-point chelate, in which two successive ligand dissociation events must take place before a catalytically active fragment is generated. Potentially, this additional donor could dramatically slow catalyst initiation (eq 6). We chose to conserve the imine donor (L) and examine relatively weak third donors (L′) in the hope that the additional point of attachment would push the

(19) Ritter, T.; Hejl, A.; Wenzel, A. G.; Funk, T. W.; Grubbs, R. H. *Organometallics* **2006**, *25*, 5740−5745.

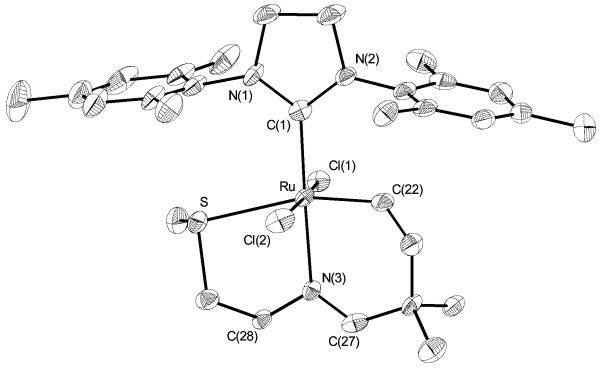

Figure 7. Solid-state structure of **17c** with thermal ellipsoids drawn at 50% probability. Selected bond distances (Å) and angles (deg): Ru−C(1) = 2.053(4), Ru−C(22) = 1.840(4), Ru−N(3) = 2.185(3), Ru−Cl(1) = 2.4023(10), Ru−Cl(2) = 2.4189(13), Ru−S = 2.5971(12), Cl(1)−Ru−Cl(2) = 172.58(4), C(1)−Ru−N(3) = 177.85(15), C(22)−Ru−N(3) = 83.15(14), C(22)−Ru−S = 163.10(11).

initiation temperatures higher, but retain the high inherent activity of the NHC−Ru framework.

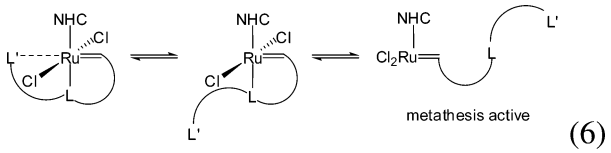

(6)

The synthesis of ligands **16a−c** was carried out analogously to **14a−e** and gave the unsaturated imine ligands containing ether and thioether groups in good yield. The catalyst synthesis was straightforward starting from **3** to give the catalysts **17a−c** in good yield (eq 7). These catalysts could be easily isolated by precipitation and were quite stable on the benchtop.

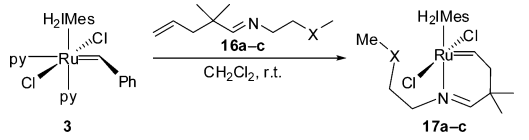

(7)

The ^{1}H NMR spectra for **17a−c** are consistent with the structures depicted in eq 7. The complexes show the characteristic alkylidene protons, which for the thioether compound are shifted slightly upfield (18.45 vs ∼18.7 ppm). Most important in these spectra is that the resonance corresponding to the terminal methyl bound to the X donor in **17b** and **17c** is significantly shifted from that in the free ligand upon complexation to ruthenium, suggesting that the extra donor is binding to the ruthenium center. The terminal methyl resonance in **17b** shifts from 3.34 to 2.83 ppm, while the corresponding resonance in **17c** shifts from 2.12 to 1.43 ppm. There is almost no shift for the resonance of the terminal methyl group in **17a**, where the butyl substituent does not interact with the ruthenium. Somewhat unexpectedly, the resonances corresponding to the H_2IMes ligand are still sharp, suggesting that the extra donor does not inhibit NHC rotation.

The structure of **17c** was determined by X-ray crystallography and is shown in Figure 7.[20] The complex shows approximate

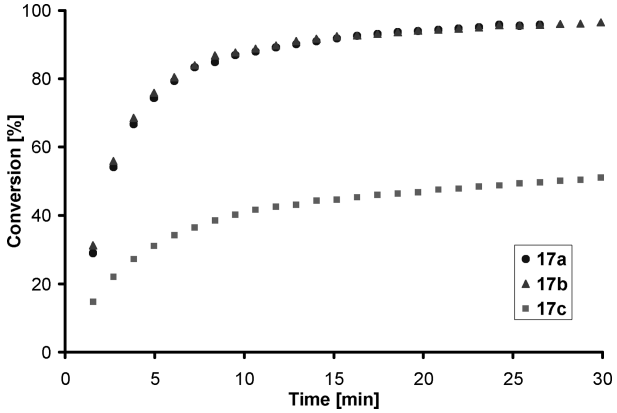

Figure 8. Conversion plot for RCM of **10** with **17a−c** (2.5 mol %, 60 °C, C_6D_6).

octahedral geometry, and the sulfur coordinates to ruthenium trans to the alkylidene. The Ru−S bonding distance (∼2.59 Å) is quite long; a search of the Cambridge Crystallographic Database shows that typical Ru−thioether bonds are in the range 2.3−2.4 Å. The long Ru−S distance in **17c** may partially be a result of its placement opposite the strongly trans-influencing alkylidene group. The Ru−N bond distance (∼2.17 Å) is longer than that observed in the other imine complexes but may be a consequence of the need to bind a third donor in a five-membered chelate ring. The bond angles for the pairs of trans ligands (H_2IMes−Ru−N(3) 177.85(15)°, Cl−Ru−Cl 172.58(14)°) are closer to an ideal 180° than in the other square pyramidal ruthenium complexes characterized here.

These 3-point chelates were tested in the RCM of **10** and found to show activity at elevated temperature (60 °C). **17a** and **17b** show essentially identical activities, which suggests that although the oxygen appears to interact with the ruthenium, it does not bind tightly enough to measurably impact the catalysis. The sulfur-containing **17c**, on the other hand, shows much lower activity for RCM, indicating that the thioether has a major impact, which is not unexpected given that sulfur is generally a better ligand for ruthenium than oxygen. NMR data show that precatalyst **17c** is still present in significant quantities during the course of the reaction, implying that the complex is not decomposing, but is just a slow initiator. The possibility of sulfur poisoning the catalyst was examined, but reactions carried out in the presence of dimethyl sulfide did not approach the change in rate observed with **17c** (see Supporting Information). Under these conditions **1** and **2** catalyze this reaction to completion within 2 min, which highlights the latency of **17a−c**. These RCM results suggest that incorporating a third point of attachment can also have a major impact on catalysis but is strongly dependent on the nature of the additional donor.

Conclusion

Catalysts featuring imine donors chelated through the alkylidene have been synthesized and studied in RCM and ROMP reactions. These catalysts show latent behavior: slow at room temperature but high activity at elevated temperatures. Similar systems also allow access to other strategies, such as the introduction of additional donors, which was shown to have a major impact on catalytic activity. We also examined the effect of relative placement of the imine bond and found that catalysts possessing an exocyclic imine bond resulted in not latent, but fast-initiating metathesis catalysts. The modular synthesis is easily adapted to modification of steric and electronic parameters, allowing for a high degree of tunability of catalyst

(20) For **17c**, four unique but similar molecules crystallize in the unit cell. The distances and angles for one molecule have been reported in the text. For complete details see the Supporting Information.

initiation. These latent catalysts could be useful in a range of high-temperature applications.

Acknowledgment. We thank Lawrence M. Henling for contributions to the crystallography and Materia, Inc. for generous donations of catalyst. This research was supported by the U.S. National Science Foundation.

Supporting Information Available: Complete experimental details for the synthesis and characterization of all new compounds, catalytic procedures, and X-ray crystallographic details and data in CIF format. This information is available free of charge via the Internet at http://pubs.acs.org.

OM060620U